THE JOURNAL OF PHYSICAL CHEMISTRY B

Article

pubs.acs.org/JPCB

Water Dynamics in Physical Hydrogels Based On Partially Hydrophobized Hyaluronic Acid

Chiara Chiapponi,[†] Maria Teresa Di Bari,*[,†] Yuri Gerelli,[‡] Antonio Deriu,[†] Ester Chiessi,[§] Ivana Finelli,[§] Gaio Paradossi,[§] Margarita Russina,[∥] Zunbeltz Izaola,[∥] and Victoria Garcia Sakai[⊥]

[†]Dipartimento di Fisica e Scienze della Terra, Università di Parma and CNISM, Parma, Italy

[‡]Institut Laue-Langevin, Grenoble, France

[§]Dipartimento di Scienze e Tecnologie Chimiche, Università di Roma "Tor Vergata", Roma, Italy

[∥]Helmholtz-Zentrum Berlin für Materialien und Energie, Berlin, Germany

[⊥]ISIS Facility, Rutherford Appleton Laboratory, Didcot, United Kingdom

ABSTRACT: The dynamics of hyaluronate-based hydrogels has been investigated by quasielastic neutron scattering (QENS). Hyaluronate (HYA) has been compared, in the same conditions of temperature and polymer concentration, to a chemically modified form, HYADD, in which the backbone has been grafted with a hexadecyl (C_{16}) side-chain with a degree of substitution of about 2% (mol/mol). This modification increases the hydrophobicity of the polysaccharide and leads to a stable gel already at polymer concentration of 0.3% (w/v), yielding a viscosupplementation with less quantity of polysaccharide. The time-scale covered by our measurements probes both water and segmental biopolymer motions. In both systems, the local dynamics of the network in the ps time-scale is mostly due to local reorientational motions of side groups. Such motions are not significantly affected by the small amount of aliphatic chains forming the hydrophobic junctions in HYADD. The diffusivity of water in both HYA and HYADD coincides with that of pure water within the experimental uncertainty. This result confirms previous ones on the dynamics of water in HYA solutions and it is of relevance for biomedical applications of hyaluronate-based systems because it affects the diffusive processes of metabolites and their interaction with tissues.

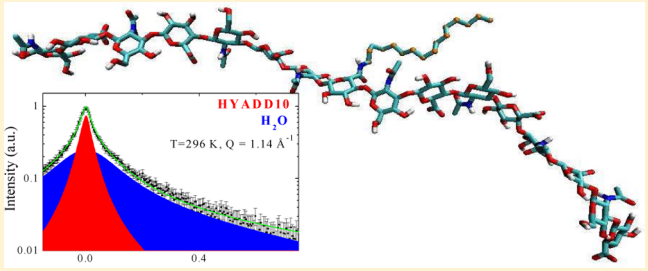

1. INTRODUCTION

Over the past years biomedical and pharmaceutical research has developed novel systems for advanced therapeutic methodologies, ranging from viscosurgery, viscosupplementation, stem cells growth, to gene therapy, targeted release of drugs, and molecular imaging. Among novel drug platforms, hydrogel matrices play an important role: they are multicomponent systems made up of an aqueous solution and a polymeric moiety, which imparts different functions to the matrix such as responsiveness to external stimuli, affinity to receptors, or controlled drug release.[1−3] Among them, macroscopic hydrogels stabilized by noncovalent interactions and based on hyaluronic acid have been studied in detail for their unique viscoelastic properties along with their biocompatibility and nonimmunogenecity.[4,5] Hyaluronate (HYA) is currently used in a number of cosmetic, medical, and pharmaceutical applications. In biomedicine, HYA has been employed as cell scaffold in tissue engineering and it is used in the treatment of osteoarticular pathologies.[6] It has also been investigated as a drug delivery agent for ophthalmic, nasal, pulmonary, parenteral, and dermal routes.

HYA is a natural polysaccharide belonging to the family of glycosaminoglycans, extracellular polymers present throughout the animal kingdom; its chains are characterized by the repetition of the disaccharide unit formed by D-glucuronic acid and D-*N*-acetylglucosamine residues connected via alternating β-1,4 and β-1,3 glycosidic bonds.

HYA is a polysaccharide with a relevant number of functionalities in nature.[3] It takes part in the building of cartilages: in the presence of proteins that regulate the aggregation processes in cartilage, HYA organizes itself in large aggregates with high charge density that are able to osmotically attract huge amounts of water in tissues. Other functions of HYA include the hydrodynamic regulation of the fluids of the extracellular matrix, cell proliferation, and mobility.

Recently, the known biospecificity of HYA for CD44, a transmembrane protein overexpressed by many types of cancer cells has been deployed for the targeting of tumor cells.[7]

Nowadays, academic and industrial laboratories are focusing on derivatives of HYA obtained by controlled chemical modifications. Among them, of relevance is HYADD, a chemically modified form of hyaluronate, which is obtained

Received: April 16, 2012
Revised: October 13, 2012
Published: October 15, 2012

by grafting hexadecylic chains to the carboxyl group of the glucuronic residue of the HYA repeating unit, with a degree of substitution (DS) between 1 and 3% mol/mol (Figure 1).[8]

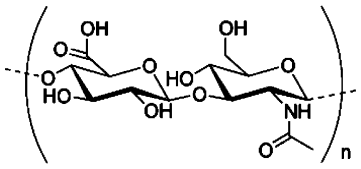

Figure 1. Molecular structure of the chemically modified hyaluronan: HYADD. The percentage of chemically modified residues is 2%.

This small chemical modification produces dramatic macroscopic effects: HYADD is able to form hydrogels at concentrations 10 times lower than those needed for natural HYA. Such a peculiarity significantly broadens applications of HYADD as compared with pure hyaluronate.

The applications of HYA gels are mostly developed on an empirical basis. A detailed description of the water−macromolecule interactions and of their role in determining the structural, dynamic, and functional properties is a necessary prerequisite to optimize hydrogel characteristics for specific applications. In hydrated polymer and biopolymer systems, hydrogen bonds are formed among water molecules, between water and the macromolecule, and among the macromolecule. The first hydration shell is closely associated with the random gel network: it affects the network mobility, enables hydrogen-bonding and proton transfer, and facilitates a plethora of biochemical processes.[9,10] In polysaccharides, for instance, a variety of complex structures can be formed depending on hydration and, therefore, on the degree of water−macromolecule association. These range from ordered fiber packing at moderate hydration levels, to dilute gels. Polysaccharide-based hydrogels are relatively stable even at very low saccharide concentration (down to 1% and less). Water may act also as a "plasticiser", inducing some degree of alignment of the saccharide units and, thus, affecting not only the conformation but also the dynamical properties at a molecular level.[11,12] Experimental results, together with data from computer simulations, have confirmed that water bound to hydrophilic sites has relaxation times lengthened compared to bulk water, assigned to an increase in the hydrogen bond connectivity in the vicinity of a hydrophilic surface.[13]

The microscopic dynamical properties of polymer- and biopolymer-based gels may cover a large time window ranging from femto- to almost microseconds. Complementary spectroscopic techniques that can altogether cover most of this interval are: NMR, dielectric relaxation, quasielastic, (QENS), and inelastic (INS) neutron scattering. Molecular dynamics computer simulations can extend the time window accessed by the spectroscopic techniques and they can also act as a guide to the interpretation of experimental data.

HYA-based gels have been studied in the past years with most of the above techniques,[14−18] but a detailed description of the dynamics of both polysaccharide chains and water solvent is still missing. We have started a systematic study at the molecular level of HYA and HYADD in order to relate local microdiffusivity properties to the peculiar macroscopic viscoelastic behavior of the HYADD gels. In this paper we report the results of a QENS investigation of the dynamics of water and of the saccharide units in the time-window ∼0.3−150 ps. The slower conformational dynamics of the whole polymeric gel scaffold will be addressed in a separate paper.

2. MATERIALS AND METHODS

HYA tetrabutylammonium salt (HYATBA), obtained from hyaluronic acid sodium salt of bacterial source (MW 7×10^5 Da) after resin ion exchange, was used as a freeze-dried powder for the synthesis of the hexadecyl derivative of HYA. Methanesulfonic acid, 1,1′-carbonyldiimidazole, hexadecylamine, o-phthaldialdehyde were supplied by Sigma and used without further purification. Dimethylsulfoxide (DMSO), methanol (MeOH), ethanol (EtOH), and phosphate-buffered solution (PBS) were RPE grade products from Carlo Erba Reagenti (Italy). Milli-Q water was used throughout this study.

2.1. Synthesis of HYADD. The synthesis of HYADD has been reported in the literature.[19] Typically, 1 g of HYATBA was dissolved at room temperature in 100 mL of DMSO, and then 30 μL of methanesulfonic acid and 26 mg of 1,1′-carbonyldiimidazole were added slowly. This activation phase was performed at room temperature while stirring for 60 min. A total of 272 mg of hexadecylamine was then added and the amidation reaction was performed at 42 °C for 16 h while stirring. A 10 mL aliquot of a saturated aqueous NaCl solution was added and the product was recovered by pouring 200 mL of EtOH into the solution and filtering the precipitate. The powder was then washed several times using a mixture of EtOH and water and finally dried in an oven. Following this procedure, 600 mg of hexadecyl-substituted HYA was obtained.

The determination of the degree of substitution was performed by HPLC/fluorimetry analysis of total hexadecylamine (HPLC system Perkin-Elmer series 200, detector Luminescent Spectr. LS30, column Versapack C18 10 μ 25 cm, mobile phase MeOH/H_2O 95/5, flow rate 1.3 mL/min) after alkaline hydrolysis (NaOH 2 M at 70 °C for 3 h while stirring), neutralization, extraction with MeOH, and derivatization of the amine with *o*-phthaldialdehyde (OPA). The fluorimetric detector was set at an excitation wavelength of 330 nm and an emission wavelength of 440 nm.

The absence of free hexadecylamine as an indicator of impurity in the reaction was confirmed by resuspending a sample of polymer in MeOH for 30 min in order to extract nonbonded amine. The collected supernatant was then treated with OPA for amine derivatization, and the hexadecylamine-OPA product was quantified using the HPLC/fluorimetry method, as described above.

The product synthesized for this study showed a degree of substitution of 2.4% mol/mol. The chemical structure was further confirmed by FT-IR and 2D-NMR spectroscopy techniques. The average molecular weight of the polymer does not decrease significantly during HYADD synthesis and formulation in the hydrogel, as determined via gel permeation chromatography with refraction index detection.

2.2. Hyaluronic Acid Hydrogel Preparation. HYADD-based hydrogels were prepared by dissolving the hexadecyl HYA derivative in phosphate buffered saline (PBS, pH 6.9) at concentrations of 10, 50, and 100 mg/mL and labeled HYADD1, HYADD5, and HYADD10, respectively. The polymer was dispersed in PBS by overnight stirring, and the milky dispersion obtained was then autoclaved for 10 min in a stoppered cylindrical glass vial. The resulting hydrogels were cooled at room temperature.

2.3. Quasielastic Neutron Experiments. QENS experiments were performed using two time-of-flight spectrometers:

the direct geometry NEAT[20] at HZB (Berlin, D) and the backscattering spectrometer IRIS[21] at the ISIS pulsed source (Didcot, U.K.). NEAT was operated at an incident wavelength of 6 Å with an energy window of −0.5 to 4 meV and an energy resolution (full width at half-maximum, fwhm) of 70 μeV. IRIS was operated in the 002 pyrolytic graphite configuration (analyzing wavelength of 6.6 Å) with an energy window from −0.3 to 1.2 meV and a 17.5 μeV resolution (fwhm). The Q-range was 0.3−1.7 Å^{-1} for both instruments.

Using two spectrometers with different energy resolution, we were able to access a dynamical window covering about 3 orders of magnitude in time (from ∼0.3 to ∼150 ps). In the IRIS spectra, quasielastic scattering contributions from both polymer and solvent can be observed owing to the large dynamic range of the instrument coupled to a high energy resolution. On the other hand, in the NEAT spectra the quasielastic broadening is due only to the solvent because polymer motions contribute to energies within the instrumental resolution.

To enhance the contribution from the internal dynamics of the gel network in the IRIS experiment, the measurements were performed on D_2O-hydrated samples, while the NEAT ones were performed on samples in H_2O buffer. The polymer concentrations c (c = weight of dry polymer/volume of the gel) considered were 1, 5, and 10% (w/v) in the case of NEAT, and 5 and 10% (w/v) in the case of IRIS. The lowest concentration was not measured on IRIS since, even in D_2O buffer, the scattering is largely dominated by the solvent and the network contribution could not be resolved with sufficient accuracy. The explored temperatures were in the range 275 − 320 K.

In Figure 2 experimental NEAT (a) and IRIS (b) spectra (after cell subtraction) are compared for HYA10 viscous solutions and HYADD10 gels. The scattering curves for the two samples are remarkably similar, and only a very small difference can be observed: the broadening in the region below ∼30 μeV is slightly smaller for HYADD10.

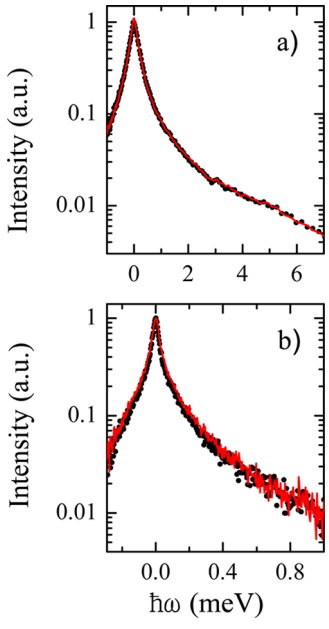

Figure 2. QENS spectra (Q = 1.15 Å^{-1}) for HYA10 (red curve) and HYADD10 (black circles) at T = 296 K measured on NEAT (a) and on IRIS (b).

3. DATA ANALYSIS

The incoherent scattering intensity is proportional to the dynamical structure factor $S(Q,\omega)$, and for HYA and HYADD samples it can be written as

$$I(Q,\omega) = A[\alpha S_p(Q,\omega) + (1-\alpha)S_w(Q,\omega)] \otimes R(Q,\omega) + bkg \quad (1)$$

where A is a normalization factor, $\alpha = \sigma_p/(\sigma_p + \sigma_w)$ is the fractional scattering intensity of the polymer expressed in terms of the scattering cross sections of the polymer, σ_p, and of the solvent, σ_w. $S_p(Q,\omega)$ and $S_w(Q,\omega)$ are the normalized scattering functions of the polymer and of the solvent, respectively; they are convoluted with the instrumental resolution $R(Q,\omega)$. An energy independent background, bkg, is also considered.

In hydrogenous polymers, the scattering intensity is mostly due to confined hydrogen dynamics. To describe these motions, we adopt a simplified model in terms of a single exponential relaxation describing the average dynamics of the hydrogens in the polymer network. The scattering law then contains an elastic term and a quasielastic one with Lorentzian line shape:

$$S_p(Q,\omega) = \left[A_0(Q)\delta(\omega) + [1 - A_0(Q)] \times \frac{1}{\pi}\frac{\Gamma_p(Q)}{\omega^2 + \Gamma_p^2(Q)}\right] \quad (2)$$

$A_0(Q)$ is the incoherent elastic structure factor (EISF) and $\Gamma_p(Q)$ is the width of the quasielastic Lorentzian.

For the water subspectrum the following expression has been adopted:

$$S_w(Q,\omega) = [S_t(Q,\omega) \otimes S_r(Q,\omega)] \quad (3)$$

where $S_t(Q,\omega)$ and $S_r(Q,\omega)$ account for the translational diffusion and the rotational dynamics of water molecules, respectively. In a strongly associated liquid like water, translational and rotational motions cannot, in general, be decoupled, and several models have been developed to go beyond the decoupling approximation.[22−24] However, these models, at temperatures close to ambient, in the Q-range analyzed here (Q < 2 Å^{-1}, i.e., below the maximum of the water structure factor) and for characteristic times up to a few picoseconds, provide lineshapes and diffusivity parameters very close to those of the decoupled roto-translational dynamics.[22,25,26] In addition, the use of the eq 3 makes it possible to directly compare the present results with older ones on similar polysaccharide gels reported in the past.[17,27]

For the translational component in eq 3 we considered a random distribution of jump lengths;[28] this leads to a Lorentzian profile:

$$S_t(Q,\omega) = \frac{1}{\pi}\frac{\Gamma_t}{\omega^2 + \Gamma_t^2} \quad (4)$$

with a Q-dependent width given by

$$\Gamma_t(Q) = \frac{D_w Q^2}{1 + D_w Q^2 \tau} \quad (5)$$

where D_w is the self-diffusion coefficient and τ denotes the residence time between jumps.

dx.doi.org/10.1021/jp303657a | J. Phys. Chem. B 2012, 116, 12915−12921

For the rotational component in eq 3 we adopted the classical Sears model of isotropic diffusion on a spherical surface of radius a.[29]

$$S_r(Q, \omega) = \frac{1}{\pi} \sum_l (2l + 1) j_l^2(Qa) \frac{l(l + 1)\Gamma_r}{\omega^2 + [l(l + 1)\Gamma_r]^2} \quad (6)$$

where $j_l(Qa)$ is the l-th order spherical Bessel function and Γ_r represents a isotropic rotational diffusion constant. In the present case, a was assumed to correspond to the O−H distance (0.942 Å).

4. RESULTS AND DISCUSSION

Typical NEAT and IRIS spectra are displayed in Figure 3a,b at the same Q (1.15 Å^{-1}) for HYA10 samples at T = 296 K; the water and polymer subspectra are also shown.

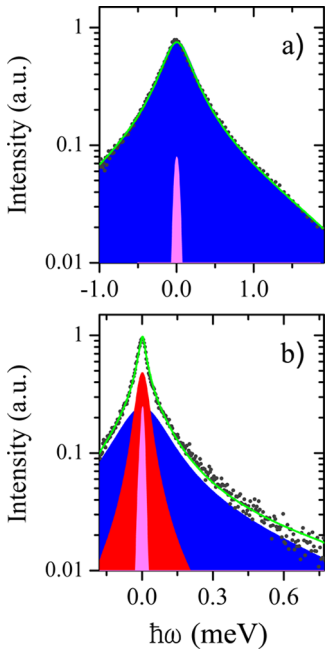

Figure 3. QENS spectra (Q = 1.15 Å^{-1}) for HYA10 at T = 296 K measured on NEAT (a) and on IRIS (b). The total fit (green curve) according to eq 1 and its components are shown: elastic peak (light magenta area), quasielastic polymer subspectrum (red area) and water subspectrum (blue area).

As remarked in section 2.3, in the NEAT spectra no quasielastic polymer contribution can be observed because its broadening is smaller than the instrument energy resolution. The polymer subspectrum can then be expressed in terms of a purely elastic line (i.e., $A_0(Q)$ = 1 in eq 2), and the total scattering function (eq 1) depends on five parameters: the normalization factor A, the polymer fractional scattering intensity α, and three water diffusion parameters: D_w, τ, and Γ_r in eqs 4−6.

The amount of water strongly bound to HYA has been investigated by adiabatic compressibility measurements,[30] as well as by differential scanning calorimetry measurements.[31,32] From these studies, 0.6−0.7 g of water per g of HYA are strongly bound to the polymer scaffolding. This value corresponds to 13−16 water molecules per repeating disaccharide unit. However, by comparing this findings with the results of molecular dynamics simulations on the structure of the hydration shell in HYA oligomers,[33] it can be inferred that only about 30% of these molecules are strongly hindered to exchange with the external water, due to the involvement in direct hydrogen bonds with HYA groups. According to this criterion, we estimated 4−5 as the number of water molecules with a dynamics close to that of the polymer chains on the time scale of QENS experiments. With this assumption, the polymer fractional scattering intensity α can be estimated on the basis of sample composition and scattering cross sections. In the case of hydrogenous gels in H_2O buffer, α = 0.007, 0.04, 0.08 for c = 1, 5, and 10%, respectively.

The values of α obtained from the fits of the NEAT spectra are in good agreement with the above estimates. The water diffusivity parameters D_w, τ, and Γ_r have been derived from the fit according to eqs 3−6. Within the experimental uncertainty, D_w and τ values obtained for HYA and HYADD coincide with those of pure water at all the measured temperatures (Figure 4).[34,35]

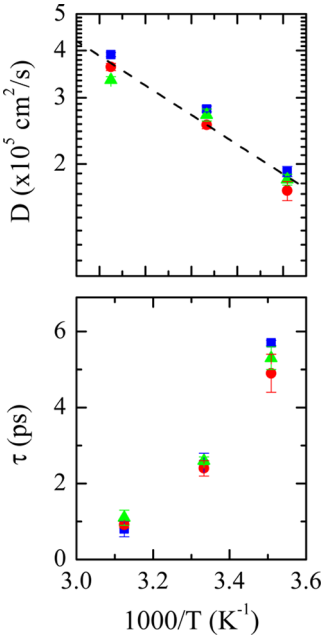

Figure 4. Diffusion coefficient (upper panel) and residence time τ (lower panel) of pure water (blue squares) and of water in HYA10 (red circles) and HYADD10 (green triangles).

Owing to the limited maximum scattering vector accessible (Q_{max} = 1.7 Å^{-1}), only the first three terms in the Sears expansion (eq 6) contribute significantly to $S_r(Q,\omega)$. From our fits, the values of Γ_r are in agreement with that of pure water[34,36] at the same temperatures; for example, at 300 K, Γ_r = (350 ± 50) μeV, corresponding to a relaxation time equal to 1.8 ± 0.3 ps.

This remarkable feature highlights that the limited structural modification in HYADD does not change the diffusional behavior of water found in the HYA dispersions, in contrast to the viscoelastic properties of HYADD gels, which greatly differ from the solutions of the parent polysaccharide at the same concentrations. A similar result has recently been reported for poly(vinyl alcohol) aqueous solution at a polymer concentration of 10% (w/v);[37] the microviscosity of poly(vinyl alcohol) was found to be comparable to that of pure water, and the rheological properties of water domains located

between macromolecules were very similar to that of pure water, although the macroviscosity of the system was strongly affected by the polymer.

As previously remarked, owing to the higher instrument resolution (ΔE = 17.5 μeV fwhm), IRIS spectra provide information on both water and polymer dynamics. To enhance the contribution from the polymer, all the samples were prepared in D_2O buffer.

The data sets have been fitted according to eqs 1−3. Preliminary fits indicated that gel water contributes to a subspectrum significantly broader than that of the polymer network. The values of the polymer fractional scattering intensity α can be calculated assuming that only water molecules making up the first hydration shell are closely associated to the gel network. For a D_2O buffer and taking into account H/D isotopic exchange between D_2O and hydroxyl groups of hyaluronate, the calculated values are α = 0.21 and 0.31 for c = 5 and 10%, respectively. The values obtained from the fit are in good agreement with these estimates.

The water subspectrum is well described by the same model used for the NEAT spectra (eqs 4−6); this is not surprising because the maximum Q explored with IRIS ($\sim$ 1.7 Å^{-1}) is lower than that of the first maximum in the structure factor of D_2O ($Q \sim$ 1.95 Å^{-1}), hence, coherence effects in the QENS spectra are not relevant. The diffusivity parameters obtained from the fit agree well with those obtained from the NEAT spectra and are very close to those of "free water". The polymer subspectra have been analyzed following two different strategies: fitting the whole spectrum with fixed fit parameters for the D_2O subspectrum or subtracting D_2O spectra, taking into account the excluded volume and the above α values. The two approaches give analogous results, and a typical polymer subspectrum is shown in Figure 5.

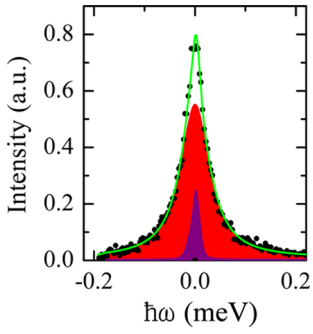

Figure 5. Fit (green curve) of the polymer spectrum according to eq 2. The elastic peak (purple area) and the quasielastic component (red area) are shown.

The polymer subspectra were fitted to eq 2 where the EISF, A_0, and the quasielastic broadening, $\Gamma_p(Q)$ are the fit parameters. In Figures 6 and 7, the values of A_0 and $\Gamma_p(Q)$ obtained from the above analysis are compared for HYA10 and HYADD10 at different temperatures. The width $\Gamma_p(Q)$ is markedly Q-dependent with an initial plateau up to ~0.7 Å^{-1} followed by a rapid increase. These broadenings involve energies in the range 0.07−0.007 meV corresponding to relaxation times ranging from 10 to 100 ps. Reorientational motions on similar time-scales have been observed in NMR measurements for oligomers of HYA in solution at 298 K.[38] They have been interpreted in terms of a superposition of a rotational tumbling of the molecule around the β-1,4−β-1,3

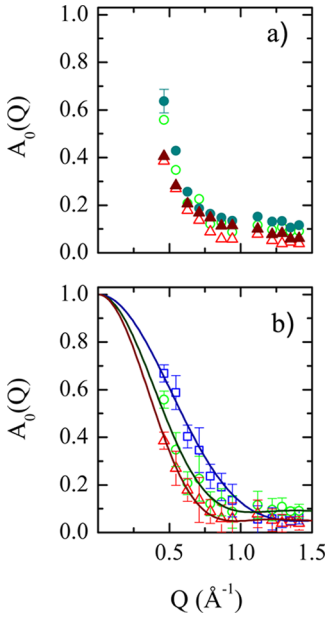

Figure 6. Q-Dependence of the EISF. (a) HYA10 (open symbols) and HYADD10 (full symbols) at 320 K (triangles) and 296 K (circles). Errors are almost constant over the explored Q-range. They are shown only for a single point to improve visibility of the different data sets. (b) Fits to eq 8 for HYA10 at T = 320, 296, and 275 K from bottom to top.

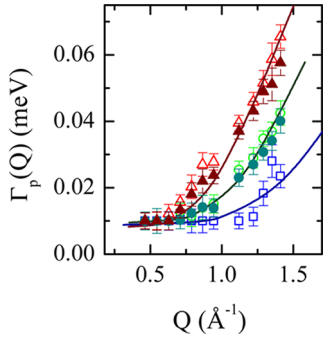

Figure 7. Q-Dependence of the quasielastic line width, $\Gamma_p(Q)$, for HYA10 (open symbols) and HYADD10 (full symbols) at T = 320 K (triangles), 296 K (circles), and 275 K (squares). Fits to eq 7 are shown as continuous lines.

vector and of a local reorientation of the C−H bond.[38−40] It is noteworthy that, in our experiment, owing to the D−H isotopic exchange that mostly occurs in hydroxyl groups, the signal from the HYA matrix is predominantly due to the same chemical groups observed in ^{13}C NMR relaxation.

Furthermore, the Q-dependence of both A_0 and $\Gamma_p(Q)$ does not change with concentration and is only slightly affected by the chemical differences between HYA and HYADD.

The observed behavior of A_0 and $\Gamma_p(Q)$ is typical of confined diffusion. To better quantify this behavior we considered a simple model of free diffusion inside a spherical volume.[41] In this case, the incoherent scattering law, $S_p(Q,\omega)$, contains an elastic term and a quasielastic one made up from a sum of Lorentzian functions $L(\lambda_n^l D_p;\omega)$. Their half-width at half-maximum, $\lambda_n^l D_p$, depends on the confined diffusion coefficient, D_p, and on the eigenvalues, λ_n^l, of the rate equation that describes the confined motion within a spherical potential:

dx.doi.org/10.1021/jp303657a | J. Phys. Chem. B 2012, 116, 12915−12921

$$S_p(Q, \omega) = [A_0(Q)\delta(\omega) + \sum_{(l,n)\neq(0,0)} (2l+1)A_n^l(Q)L(\lambda_n^l, D_p; \omega)] \quad (7)$$

For this model the EISF turns out to be

$$A_0(Q) = f + (1-f)\left[\frac{3j_1(QR_p)}{QR_p}\right]^2 \quad (8)$$

where f is the fraction of hydrogens that do not contribute to the confined dynamics and R_p is the radius of the confining volume: it can be considered as the average distance between sites occupied by hydrogens during the rotational tumbling of the HYA monomer. The IRIS data for the polymer subspectra have then been fitted to eqs 7 and 8. The parameter values resulting from the fits are summarized in Table 1. In the temperature range investigated, almost all hydrogens take part to the confined diffusion (i.e., $f = 0$ within the experimental error). The values of the diffusion coefficient, D_p for HYA and HYADD coincide within the experimental accuracy. The temperature dependence of both D_p and R_p can be described by an Arrhenius law with similar activation energies $E_a \sim 4.8$ kJ mole^{-1}; this value is close to those obtained by different spectroscopies (NMR, ESR, fluorescence depolarization, dielectric relaxation) for relaxation processes of local groups in polymer systems.[42]

Table 1. Parameters Resulting from the Fit of HYA and HYADD Polymer Subspectra According to the Volino Model (eqs 7 and 8)

T (K)	f	R_p (Å)	D_p ($\times 10^5$ cm^2/s)
275	0.1(1)	3.2(1)	0.34(5)
296	0.1(1)	4.2(1)	0.49(6)
320	0.1(1)	4.6(1)	0.65(7)

In Figure 6b, the EISF, $A_0(Q)$, is shown for HYA10 at different temperatures. The points are the experimental values of $I_{el}/I_{el} + I_{qens}$, the continuous lines are obtained from eq 8 with the values of f and R_p obtained from the fit. For the same sample, the broadening of the quasielastic component (HWHM) is shown in Figure 7. The points are obtained from the fit of the polymer subspectra to eq 2, the continuous lines are evaluated from the sum of the Lorentzian lineshapes in eq 7.

5. CONCLUSIONS

HYA is a biopolymer of primary scientific interest owing to an expanding variety of applications in cosmetic and biomedical fields. Research is attempting to improve biotechnological production processes and also to develop new HYA formulations and HA-based new materials.[43] Despite the fact that the unusual and distinctive properties of HYA polymer solutions were first established many decades ago, we are still far apart from a comprehensive knowledge of HYA and HYA derivatives. Only recently, with the application of advanced spectroscopic techniques, their molecular behavior at the local and atomic level is being better defined. This can lead to a clearer understanding of how the peculiar macroscale properties are related to the interaction of the local polymer structure with the water and ions that surround it. In the present study, using two neutron spectrometers with different energy resolution, we have compared the microscopic dynamics of HYA semidilute solutions with that of a typical chemical derivative (HYADD) that makes it possible to obtain relatively stable gels even at very low polymer concentration (<0.3% by weight). The time window accessed (~ 0.3−150 ps) is relevant for both water and local reorientational motions of side groups of the biopolymer network.

The diffusivity of water in HYA and HYADD matrixes coincides with that of pure water within the experimental uncertainty. This result confirms earlier ones on the dynamics of HYA gels[17] and it can be understood considering the very large average pore size (typically a few thousand Å) in both gels as well as the reversible character of the physical junction domains stabilizing the matrix. At the investigated concentrations, the amount of water closely bound to the gel scaffolding (first hydration shell: ~ 4−6 water molecules per saccharide dimer) is small and its contribution to the spectra cannot be distinguished from that of the saccharide chains.

The local dynamics of the gel network in the ps time-scale is mostly due to local reorientational motions of side groups. They can be modeled in terms of diffusion in a confined volume with a typical size of few Angstrom; the activation energy of the confined diffusivity is close to that of local relaxation processes in long polymer chains.[39] Such motions are not significantly affected by the small amount of aliphatic chains forming the hydrophobic junctions in HYADD: the two systems therefore show a very similar behavior. Looking at Figures 5 and 6, only a very small systematic difference is visible between HYA and HYADD data: lower quasielastic broadenings and higher EISF values indicating an overall greater stiffness of the hydrogel obtained by the hydrophobized hyaluronan, HYADD.

Larger dynamic differences should be expected at long times ($t > 1$ ns) and at scale lengths comparable with those of the average spacing between alkyl side chains (about 500 Å) along the polysaccharide chain. To access this time−space region, we have performed high resolution QENS experiments using high-resolution backscattering and spin−echo spectrometers. The results will appear in a subsequent paper.

The similar dynamic behavior of water in both polysaccharide-based matrixes is an important asset for the use of HYADD hydrogels as a functional viscosupplement. The viscoelastic properties shown by this matrix, greatly different from those displayed by the parent hyaluronan chains, leave unaltered the microscopic dynamic features of water which control the microdiffusivity of metabolites through the hydrogels and preserve the structural integrity of the macromolecular species contained in the joints cartilage.

AUTHOR INFORMATION

Corresponding Author

*E-mail: mariateresa.dibari@fis.unipr.it.

Notes

The authors declare no competing financial interest.

ACKNOWLEDGMENTS

This work was partially funded by MIUR PRIN Project 20077LCNTW. HYADD sample was kindly provided by Drs. Davide Renier and Devis Galesso of FIDIA Farmaceutici SpA, Abano Terme, Padova, Italy. The NEAT experiment has been supported by the European Commission under the Seventh Framework Programme through the Key Action: Strengthening

the European Research Area, Research Infrastructures, Contract No. 226507(NMI3). The IRIS experiment was performed within Agreement No. 01/901 between CCLRC and CNR.

REFERENCES

(1) Akiyoshi, K.; Sunamoto, J. *Supramol. Sci.* **1996**, *3*, 157−163.
(2) Sunamoto, J.; Sato, T.; Taguchi, T.; Hamazaki, H. *Macromolecules* **1992**, *25*, 5665−5670.
(3) Akiyoshi, K.; Deguchi, S.; Moriguchi, N.; Yamaguchi, S.; Sunamoto, J. *Macromolecules* **1993**, *26*, 3062−3068.
(4) Liao, Y. H.; Jones, S. A.; Forbes, B.; Martin, G. P.; Brown, M. B. *Drug Delivery* **2005**, *12*, 327−342.
(5) Falcone, S. J.; Palmeri, D.; Berg, R. A. *Polysaccharides for Drug Delivery and Pharmaceutical Applications*; ACS Symposium Series, American Chemical Society: Washington, DC, 2006; Vol. *934*, ch. 8, pp 155−174.
(6) Anand, A.; Balduini, F.; Rogers, K. *Eur. J. Orthop. Surg. Trauma.* **2010**, *20*, 645−649.
(7) Aruffo, A.; Stamenkovic, I.; Melnick, M.; Underhill, C. B.; Seed, B. *Cell* **1990**, *61*, 1303−1313.
(8) Finelli, I.; Chiessi, E.; Galesso, D.; Renier, D.; Paradossi, G. *Macromol. Biosci.* **2009**, *9*, 646−653.
(9) Jeffrey, G. A.; , Saenger, W. *Hydrogen Bonding in Biological Structures*; Springer-Verlag: Berlin/New York, 1991.
(10) Zimmerman, S. B.; Minton, A. P. *Annu. Rev. Biophys. Biomol. Struct.* **1993**, *22*, 27−65.
(11) French, D. In *Starch: Chemistry and Technology*, 2nd ed.; Whistler, R. L., BeMiller, J. N., Paschall, E. F., Eds.; Academic Press: New York, 1984; pp 183−247.
(12) Di Bari, M.; Cavatorta, F.; Deriu, A.; Albanese, G. *Biophys. J.* **2001**, *81*, 1190−1194.
(13) Weiss, W. *J. Phys. (Paris)* **1987**, *48*, 877−883.
(14) Cavalieri, F.; Chiessi, E.; Paci, M.; Paradossi, G.; Flaibani, A.; Cesàro, A. *Macromolecules* **2001**, *34*, 99−109.
(15) Průsová, A.; Conte, P.; Kucerík, J.; Alonzo, G. *Anal. Bioanal. Chem.* **2010**, *397*, 3023−3028.
(16) Vuletić, T.; Dolanski Babić, S.; Ivek, T.; Grgičin, D.; Tomić, S. *Phys. Rev. E* **2010**, *82* (011922), 1−10.
(17) Deriu, A. In *Biological Macromolecular Dynamics*; Cusack, S., H. Büttner, Ferrand, M., Lagan, P., Timmins, P., Eds.; Adenine Press: New York, 1997; pp 135−142.
(18) Kaufmann, J.; Möhle, K.; Hofman, H.-J.; Arnold, K. *J. Mol. Struct.: THEOCHEM* **1998**, *422*, 109−121.
(19) Fidia Farmaceutici, S.p.A.; Schiavinato, A.; Bellini, D. Patent *US 0069884 A*, 2008.
(20) www.helmholtz-berlin.de/user/neutrons/instrumentation/neutron-instruments/v3/index_en.html.
(21) http://www.isis.stfc.ac.uk/instruments/iris/.
(22) Di Cola, D.; Deriu, A.; Sampoli, M.; Torcini, A. *J. Chem. Phys.* **1996**, *104*, 4223−4232.
(23) Di Bari, M.; Deriu, A.; Sampoli, M. *Phys. B* **1999**, *266*, 92−96.
(24) Faraone, A.; Liu, L.; Mou, C.; Shih, P.; Copley, J. R. D.; Chen, S. H. *J. Chem. Phys.* **2003**, *119*, 3963−3971.
(25) Harpham, M. R.; Ladanyi, B. M.; Levinger, N. E.; Herwig, K. W. *J. Chem. Phys.* **2004**, *121*, 7855−7868.
(26) Liu, L.; Faraone, A.; Mou, C.; Yen, C. W.; Chen, S. H. *J. Phys.: Condens. Matter* **2004**, *16*, S5403−S5436.
(27) Middendorf, H. D.; Di Cola, D.; Cavatorta, F.; Deriu, A.; Carlile, C. J. *Biophys. Chem.* **1994**, *53*, 145−153.
(28) Egelstaff, P. A. *An Introduction to the Liquid State*; Academic: London, 1967.
(29) Sears, V. F. *Can. J. Phys.* **1967**, *45*, 237−254.
(30) Yoshida, H.; Hatakeyama, T.; Hatakeyama, H. In *Cellulose*; Kennedy, J. F.; Phillips, G. O., Williams, P. A., Eds., Horwood: Chichester, U.K., 1990; pp 305−310.
(31) Joshi, N. H.; Topp, E. M. *Int. J. Pharm.* **1992**, *80*, 213−225.
(32) Jouon, N.; Rinaudo, M.; Milas, M.; Desbrières, J. *Carbohydr. Polym.* **1995**, *26*, 69−73.
(33) Almond, A.; Brass, A.; Sheehan, K. *J. Phys. Chem. B* **2000**, *104*, 5634−5640.
(34) Teixeira, J.; Bellisent-Funel, M. C.; Chen, S. H.; Dianoux, A. J. *Phys. Rev. A* **1985**, *31*, 1913−1917.
(35) Qvist, J.; Schober, H.; Halle, B. *J. Chem. Phys.* **2011**, *134*, 144508(1−20).
(36) Sposito, G. *J. Chem. Phys.* **1981**, *74*, 6943−6949.
(37) Krise, K. M.; Hwang, A. A.; Sovic, D. M.; Milosavljevic, B. H. *J. Phys. Chem. B* **2011**, *115*, 2759−2764.
(38) Donati, A.; Magnani, A.; Bonechi, C.; Barbucci, R.; Rossi, C. *Biopolymers* **2001**, *59*, 434−445.
(39) Furlan, S.; La Penna, G.; Perico, A.; Cesàro, A. *Macromolecules* **2004**, *37*, 6197−6209.
(40) Nestor, G.; Kenne, L.; Sandström, C. *Org. Biomol. Chem.* **2010**, *21*, 2795−802.
(41) Volino, F.; Dianoux, A. J. *Mol. Phys.* **1980**, *41*, 271−279.
(42) Bahar, I.; Erman, B. *Macromolecules* **1987**, *20*, 2310−2311.
(43) Burdick, J. A.; Prestwich, G. D. *Adv. Mater.* **2011**, *23*, H41−H56.